derived on the basis of curve T can be shown to be consistent with that deduced from the non-thermal radio spectrum in the Galaxy.

Half of the observed nucleons, belonging to the old component, is shared among various nuclear species approximately in proportion to the respective interaction mean-free paths. The estimated percentages of the old component among the observed p, He, (C+O), (F to Sc), (P to Cr) and (Fe Group) nuclei are respectively 58, 21, 9, 6, 4 and 3. Note that the new component constitutes >90% of the observed flux for nuclei other than p and He. Therefore, one can explain the observed energy dependence of the abundance ratio of secondary to primary nuclei using MLBM or NLBM for the new component. Further, the relative abundances of heavy nuclei of charge ≥6 would not differ from other models by more than a few per cent.

We now need to choose between MLBM and NLBM for the new component. According to MLBM, the energy spectrum of nucleons of recent origin above ≈8 GV/c (≈4 GeV/n) would be steeper than the injection spectrum by a power-law spectral index of about 0.5; the old component retains the injection spectrum. This would mean that the old component would dominate the observed flux beyond a certain energy[20]. The calculated energies at which the intensities from these two components become comparable are ~56, 460 and 1,950 GeV/n for He, (C+O) and (Fe group) respectively; protons have 58% old component even below 8 GeV. This clearly indicates that the observed similarity in the spectral shape of p and He above a few GeV/n cannot be understood, unless protons are accelerated differently. One should also expect a flattening of He spectrum beyond about 50 GeV/n, which has not been observed at least up to a few hundred GeV/n. These two inconsistencies discredit MLBM, and the natural choice is for NLBM, because the spectral shape of the new component is the same as the old.

A reliable estimate of the abundance of deuterium can be made using this model at relativistic energies. The estimated D/He ratio from this model is nearly twice as much from other models at energies ≤4 GeV/n and decreases slightly at high energies due to the energy-dependent confinement of the recent component in source regions. A similar enhancement is expected in the case of $^3$He abundance. The available measurements have been restricted to energies ≤200 MeV/n and these results differ by a large factor[21]. However, they can be easily detected at relativistic energies using magnetic spectrometry[22]. The observation of an enhanced abundance of D would not only confirm the predictions of this model but would also reduce the difficulty in understanding the observed charge ratio of muons at sea level. Perhaps the distribution and spectral shape of high-energy $\gamma$ rays, and the extended nonthermal radio emission in the Galaxy might also be explained by this model.

I thank Professors M. V. K. Apparao, R. R. Daniel and P. V. Ramana Murthy for helpful criticisms.

Received 15 September; accepted 10 November 1980.

1. Golden, R. L. *et al. Phys. Rev. Lett.* **43,** 1196–1199 (1979).
2. Badhwar, G. D. *et al. Nature* **274,** 137–139 (1978).
3. Smoot, G. F., Buffington, A. & Orth, C. D. *Phys. Rev. Lett.* **35,** 258–261 (1975).
4. Gaisser, T. K. & Maurer, R. H. *Phys. Rev. Lett.* **30,** 1264–1267 (1973).
5. Badhwar, G. D., Golden, R. L., Brown, M. L. & Lacy, J. L. *Astrophys. Space Sci.* **37,** 283–300 (1975).
6. Szabelski, J., Wdowczyk, J. & Wolfendale, A. W. *Nature* **285,** 386–388 (1980).
7. Stephens, S. A. *Astrophys. Space Sci.* (in the press).
8. Orth, C. D., Buffington, A., Smoot, G. F. & Mast, T. S. *Astrophys. J.* **226,** 1147–1161 (1978).
9. Juliusson, E., Mayer, P. & Muller, D. *Phys. Rev. Lett.* **29,** 445–448 (1972).
10. Cowsik, R. & Wilson, L. W. *Proc. 13th int. Cosmic Ray Conf.* **1,** 500–505 (1973).
11. Bogomolov, E. A. *et al. Proc. 16th int. Cosmic Ray Conf.* **1,** 330–335 (1979).
12. Daniel, R. R. & Stephens, S. A. *Bull. astr. Soc. Ind.* (in the press).
13. Rasmussen, I. L. & Peters, B. *Nature* **258,** 412–413 (1975).
14. Badhwar, G. D. & Stephens, S. A. *Proc. 15th int. Cosmic Ray Conf.* **1,** 398–403 (1977).
15. Badhwar, G. D. & Stephens, S. A. *Phys. Rev.* D **14,** 356–358 (1976).
16. Buffington, A., Orth, C. D. & Mast, T. S. *Astrophys. J.* **226,** 355–371 (1978).
17. Fanselow, J. L., Hartman, R. C., Hildebrand, R. H. & Mayer, P. *Astrophys. J.* **158,** 771–780 (1969).
18. Golden, R. L. *et al.* Preprint PSL-PE00947 (1979).
19. Buffington, A. & Orth, C. D. *Astrophys. J.* **199,** 669–679 (1975).
20. Peters, B. & Westergaard, N. J. *Astrophys. Space Sci.* **48,** 21–46 (1977).
21. Daniel, R. R. & Stephens, S. A. *Space Science Review* **17,** 45–158 (1975).
22. Badhwar, G. D., Stephens, S. A. & Golden, R. L. *Proc. 14th int. Cosmic Ray Conf.* **9,** 3183–3187 (1975).

# Expanding haloes in cometary comae

**W.-H. Ip**

Max-Planck-Institut fur Aeronomie, D-3411 Katlenburg-Lindau 3, FRG

**Observations indicate that cometary activity can be rather violent. Flare-ups, sunward-pointing jets and periodic formation of concentric haloes expanding outwards can also be persistent features in some comets. For example, a halo structure was observed in the coma of Comet Halley during its last visit[1]. It is argued here that halo formation may be related to the propagation of shock pairs driven through the cometary atmosphere as a result of spin-modulation of the cometary outgassing rate. Even though the non-stationary process could be less dramatic than the example considered here, its effect on the chemistry and expansion of the neutral gas as well as dynamics of the cometary plasma must be significant.**

Although theoretical models of cometary coma generally assume that neutral atmospheres expand spherically, symmetrically and without time variation, inhomogeneous structures have often been observed in the cometary comae. These include the formation of concentric shells (or haloes) moving outwards from the central source in succession and the appearance of fans or jets. Such non-stationary behaviour has long been thought to be related to the spin-modulation of the outgassing rate from the cometary nucleus[2,3].

There are two possiblities. If the surface composition of the cometary nucleus is uniform, the dependence of the surface temperature on the angle of insolation ($\theta$) would mean higher gas emission rate at the point shifted from the sunlit position with $\theta = 0°$. (The exact position of the 'hot spot' is determined by the direction and period of the nuclear spin as well as thermal properties of the surface material; the resultant jet effect has been used to explain the nongravitational acceleration or deceleration of comets[2].) As the jetting of the volatile gas—though localized—is more or less constant, the expansion of the cometary atmosphere, except the persistent sunward jets, should show no marked time variation. On the other hand, if the surface of the cometary nucleus can be divided into one active hemisphere and an inactive one (say), there will be more violent ejection of the volatile gas every time the active region turns towards the Sun. In the extreme case, there will be regular outbursts at the centre with a period equal to that of the spin period leading to large spatial and temporal variations in the structure of the coma. Clearly, the formation of expanding haloes as seen in the case of Comet Donati in 1858 (ref. 4) and Comet Halley[1] must be somehow related to such periodic outbursts. (From measurements of their respective halo structures, Whipple[5,6] has determined the spin period of Comet Donati to be 4.6 h and for Comet Halley to be 10.3 h.)

To understand this phenomenon, time-dependent expansion of the gas outflow must be considered. Here it is assumed that the cometary atmosphere is an ideal gas and that the radial expansion is spherically symmetric. Furthermore, the time variation of the outgassing rate is approximated by a step function and we are basically interested in the initial propagation of the cometary neutral gas as the strong source is switched on. If $\rho$ is the density, $u$ the radial velocity, $p$ the pressure and $\gamma(=5/3)$ the ratio of specific heats of the gas, then

$$\frac{\partial \rho}{\partial t}+\frac{1}{r^2}\frac{\partial}{\partial r}(r^2\rho u)=0 \quad (1)$$

$$\frac{\partial u}{\partial t}+u\frac{\partial u}{\partial t}=-\frac{1}{\rho}\frac{\partial p}{\partial r} \quad (2)$$

$$\frac{\partial}{\partial t}\left(\frac{p}{\rho^\gamma}\right)+u\frac{\partial}{\partial r}\left(\frac{p}{\rho^\gamma}\right)=0 \quad (3)$$

0028-0836/81/040269—03$01.00

for the hydrodynamic equations of expansion of the neutral gas from a point source. Introducing the similarity variable[7],

$$\eta = r/\alpha t \tag{4}$$

for the expansion of a piston gas with a constant speed $\alpha$ and defining

$$u = rV(\eta)/t, \quad \rho = \rho_0 r_0^2 \sigma(\eta)/r^2, \quad p = \rho_0 r_0^2 \pi(\eta)/t^2 \tag{5}$$

with the density distribution of the cometary coma at $t \leq 0$ given as:

$$\rho = \rho_0 r_0^2 / r^2 \tag{6}$$

(that is, $\rho = \rho_0$ at $r = r_0$ for the unperturbed flow), we can find an equivalent set of equations for $V$, $\sigma$ and $\pi$ with $\eta$ as the sole variable. As discussed by Simon and Axford[8], similarity solutions of $V$, $\sigma$ and $\pi$ can be obtained for the motion of such a piston gas describing a pair of shocks ($S_+$ and $S_-$) separated by a contact surface ($C$). The characteristics of the strong-shock solutions are that at the contact surface with $\eta \cong 0.84$, $V = 1$, $\pi = 0$ and $\sigma \to \infty$; and that the mass efflux from the source can be expressed as

$$Q = 4\pi f \alpha \rho_0 r_0^2 \tag{7}$$

where $f \approx 0.4$ in the case of strong shocks. With $V$, $\sigma$ and $\pi$ known for $\eta \geq 0$, the physical quantities $u$, $\rho$ and $p$ can be derived in turn for various values of $r$ and $t$ from equation (5).

Details of the similarity solutions for a blast wave can be found in ref. 8 and numerical solution of the above adiabatic non-steady flow equations in ref. 9. For brevity, only radial variation of the mass density will be discussed here. Figure 1 shows the profile of the gas density ($\rho$) plotted for the case of strong forward ($S_+$) and reverse ($S_-$) shocks. As $\sigma \to \infty$ at the contact surface ($C$), $\rho$ increases to a large value also. For weaker shocks, the snow-plow effect of piling up the material between $S_+$ and $S_-$, though less pronounced, should be present. The similarity solutions of the piston gas apply only to the inner coma region which is still dominated by collisional effect. For a Halley-type comet with a nuclear radius ($r_n$) of 3 km and a surface number density ($n_0$) of $3 \times 10^{12}$ cm$^{-3}$, the nominal dimensions of such collision zone ($r_c$) is $\approx 1.4 \times 10^4$ km. As a result of the varying outgassing rate, $r_c$ could be a factor of 3 larger or one-third smaller as the comet rotates around. Even with the large value of $4 \times 10^4$ km, $r_c$ is still small compared with the radius of outer haloes ($\sim 3 \times 10^5$ km) (see ref. 1). The compression effect by the piston gas must then stop a long way inside. However, the sharp definition of the haloes may still be maintained at large distances if the temperature of the gas at the contact surface is kept sufficiently low by collisional cooling. The delineation of the haloes is also helped by the rare-fraction region just behind the reverse-shock $S_-$. Indeed, the density variations as shown in Fig. 1 may explain why in some cases a dark zone is observed[4] immediately behind a halo of enhanced brightness. Another effect is that the propagation speed of these haloes could be considerably lower than the value of 1 km s$^{-1}$ generally quoted as the flow speed of the neutral gas in the inner coma close to the nucleus ($r \leq 10^{2-3}$ km) could be very small.

The dimension of these haloes as observed in the $C_2$-emission are limited by the scale length of these molecules ($\approx 10^5$ km at 1 AU). Furthermore, the daughter fragments of the parent molecules (such as $H_2O$ and CO) in the compressed shells would pick up extra kinetic energy during photodissociation or ion-molecular reactions such that the corresponding thin-shell structures would be dispersed. Therefore, expanding haloes are not likely to be seen in the density distributions of H, C and O atoms, for example. We may then envisage the formation of a new spherical halo moving outwards every time the active hemisphere of the cometary nucleus faces the Sun. Partly due to the pile-up of material between the forward and reverse shocks, and partly due to the projection effect along the line-of-sight, a concentric halo will be observed progressing outwards. Note that the time variation of the outgassing rate could be anything but a step function as adopted here and the shock velocity $\alpha$ should have certain time variation. The dynamical process, however, is not likely to vary much as long as the active hemisphere of the comet can produce a strong driver gas. The real issue is, therefore, what is the energy source for such outbursts if they indeed are explosive.

In connection with the flare-ups of cometary activities sometimes observed, Donn and Urey[10] have suggested that explosive chemical reactions involving free radicals or unstable molecules on the nuclear surface may provide the answer. The free-radical reactions studied in the laboratory are observed to be highly exothermic, yielding a heat of reaction of approximately a few electron volts per molecule. This would mean that there are pockets of unstable chemical mixture on the surface of the active hemisphere with energetic explosions triggered by solar radiation. Another possibility suggested by Greenberg[11] in the case of interstellar grains—is simply that some of the solid grains could release free energy stored in the mantle of organic molecules and free radicals through breakup of the cometary grains. Although highly uncertain, it is, nevertheless, interesting to look into the energy budget of the coma expansion. Taking the radial speed to be 1 km s$^{-1}$, the kinetic energy is then only of the order of 0.1 eV per $H_2O$ molecule and about $\dot{E} \approx 10^{28}$ eV s$^{-1}$ in total if the gas production rate is $\approx 10^{29}$ $H_2O$ molecules s$^{-1}$. An equivalent amount of chemical-energy source could be obtained if the sublimating ice contains 3% or so of the highly volatile material capable of exothermic chemical reaction. The energy budget of the halo expansion is therefore not a serious problem. In other words, even if the gas production rate were the same over one spin period, the contamination of one side with exothermic material would result in high-speed ejecta driving a shock pair periodically.

The hydrodynamics of the neutral coma in the inner region is not well understood. Various possible flow patterns including shock formation in steady-state conditions have been considered (see refs 12 and 13). The time-dependent expansion of the

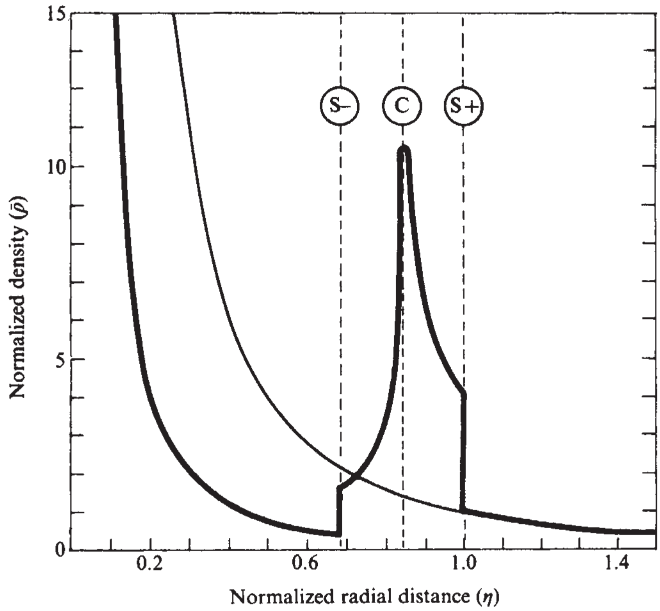


**Fig. 1** The halo formation in the cometary comae through the compression effect of a piston shock. Radial variations of the density ($\bar{\rho}$) of the cometary neutral atmosphere normalized to the corresponding value at the position of the forward shock ($S_+$) at $\eta = 1$. Therefore $\bar{\rho} = \sigma(\eta)/\eta^2$ for $\eta = 1$ and $\bar{\rho} = 1/\eta^2$ for $\eta > 1$. The value of $\sigma(\eta)$ is obtained by taking a similarity solution to equations (1)–(6) with strong shocks (see ref. 8). The brightness enhancement in the haloes is caused by the density compression between the forward and reverse shocks. The dark zone sometimes observed immediately behind the haloes could be the manifestation of the rare-fraction region behind $S_-$ as indicated. The density profile not modified by the shock pair is depicted by the thin curve.

cometary atmosphere should be even more complicated. Some idea can be derived from Bobrovnikoff's record of Comet Halley[1] where the expansion speed of the halo is estimated to be $\approx 0.25$–$0.5\ km\ s^{-1}$. Identifying this value as the propagation speed of the contact surface and using the relation that the flow speed $u^*$ behind the reverse shock should be larger by a factor of 2.5[8], we obtain $u^* \approx 0.65$–$1.3\ km\ s^{-1}$. This would mean that an additional energy source amounting to $\dot{E}^* \approx \frac{1}{2}Q(u^*)^2 \approx 10^{28}\ eV\ s^{-1}$ (for $Q \approx 10^{29}\ H_2O$ molecules $s^{-1}$) is needed to drive the piston gas. This requirement can be accommodated by introducing a small fraction of exothermic volatile material into the sublimating gas.

Whether any of these mechanisms may provide the energy required to drive a shock through the cometary atmosphere remains to be seen. But high-speed HCN jets ($u \geq 5\ km\ s^{-1}$) have been detected in the coma of Comet Kohoutek (1973f) by Huebner *et al.*[14], who also favoured explosive chemical reactions as the origin of these jets. Thus the formation of shock pairs together with a compression region in between must be considered a viable explanation for the expanding haloes. For illustration and simplicity we have considered only the strong-shock case for the similarity solutions. Other types of compression processes with weaker shocks must also exist; the present interpretation, nevetheless, highlights the nature of non-steady expansion of the cometary atmosphere.

Received 28 July; accepted 14 November 1980.


1. Bobrovnikoff, N. T. *Univ. Calif. Publ. Lick Obs.* **17,** 2 (1931).
2. Whipple, F. L. *Astrophys. J.* **111,** 375 (1950).
3. Sekanina, Z. *Icarus* **37,** 420 (1979).
4. Rahe, J., Donn, B. & Wurm, K. *Atlas of Cometary Forms* (NASA SP-198, 1969).
5. Whipple, F. L. *Nature* **272,** 134 (1978).
6. Whipple, F. L. *IAU Circ.* No. 3459 (1980).
7. Courant, R. & Friedrichs, K. O. *Supersonic Flow and Shock Waves* (Interscience, New York, 1948).
8. Simon, M. & and Axford, W. I. *Planet. Space Sci.* **14,** 901 (1966).
9. Hundhausen, A. J. *J. geophys. Res.* **78,** 1528 (1973).
10. Donn, B. & Urey, H. C. *Astrophys. J.* **123,** 339 (1956).
11. Greenberg, J. M. *Moon & Planets* **20,** 15 (1979).
12. Shul'man, L. M. in *Physics of Comets* (ed. Konopleva, V. P.) 84 (transl. NASA TT F-599, 1969).
13. Mendix, D. A. & Ip, W.-H. *Astrophys. Space Sci.* **39,** 335 (1976).
14. Huebner, W. F., Snyder, L. E. & Buhl, D. *Icarus* **23,** 580 (1974).


# Blocking highs over Asia and monsoon droughts over India


**C. R. V. Raman**

MONEX, New Delhi-3, India

**Y. P. Rao**

B3/33 Azad Apartments, New Delhi-3, India


**Severe summer droughts of the Indian subcontinent have been found to accompany prolonged 'breaks' in the south-west monsoon. Data from the years of severe drought suggest that the associated breaks were due to upper tropospheric blocking ridges over East Asia. We present here a model for the evolution of two such blocking ridges: the East Asia (EABR) and the West Asia (WABR). Apparently an intense WABR—the initiator of the monsoon break—precedes the formation of the EABR. This cycle could be a way of predicting years of intense drought or monsoon activity.**

For a long time, studies of monsoon breaks were confined to changes in circulation in the monsoon area. Ramaswamy[1–3] was the first to associate breaks with the low index circulation in middle latitude westerlies and the elongation of mid-tropospheric westerly troughs into India. However, eastward-moving westerly troughs penetrating into northern India enhance monsoon activity, and Ramanathan[4] had visualized that migrating middle latitude ridges influence monsoon onset. Examining the severe droughts of 1979 (MONEX), 1972, 1966 and 1965, Raman *et al.*[5] found that the breaks in these years were associated with stagnant upper tropospheric blocking ridges over the east Asia along ~100°E, extending from 35°N to 70°N. In such situations, westerly troughs do not move beyond 80°E and instead tend to extend southwards.

Cold lows form south-west of the EABR and the lower tropospheric monsoon trough over India gets displaced northwards into the Himalayas—the most significant characteristic of breaks. We suggest that an upper trophospheric WABR along ~50°E is a necessary precursor to the development of the EABR. Also that in drought years, a well-marked surface high appears over USSR centred at 55°N and 50°E. This surface high is linked by a ridge with the Azores High over the central Atlantic. The surface high over the USSR, overlain by a ridge of up to 100 mbar, is due to the WABR. In contrast, in good monsoon years, the surface high and the associated upper ridge over the USSR are notably absent. Instead, a trough from the Aleutian low extends into Siberia with several low centres. Such a configuration is akin to the normal pattern.

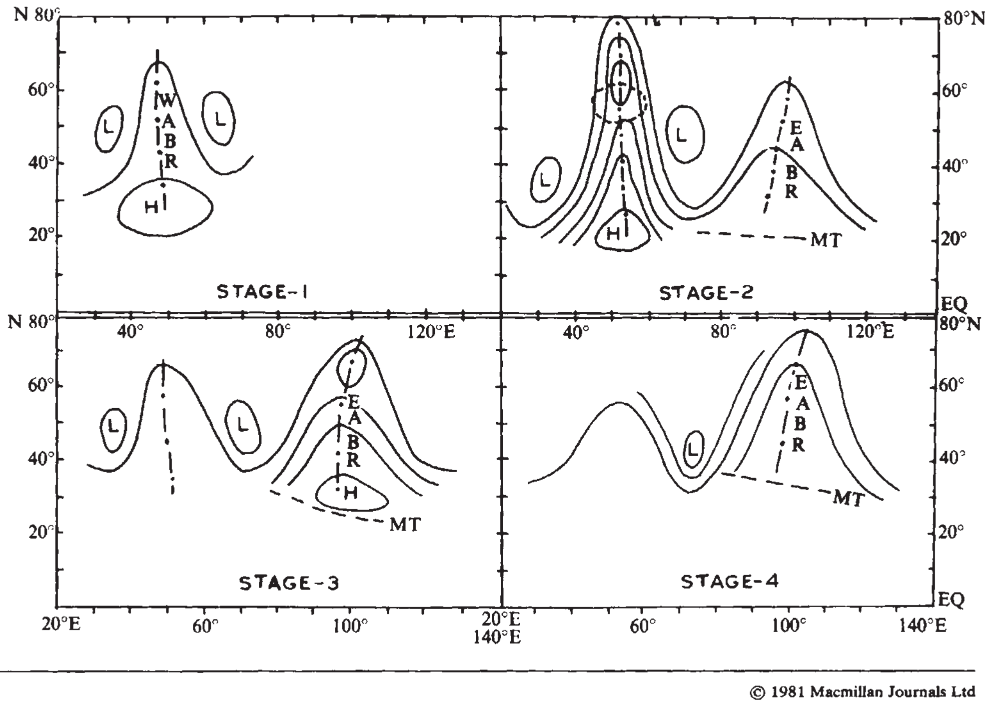


**Fig. 1** Evolution of the WABR and the EABR. Solid lines denote 200-mbar contours; H, high; L, low; dashed-dotted line indicates north–south orientation of the 200-mbar blocking ridge. Stage 1, Appearance of WABR. Stage 2, Maximum phase of WABR with intense cold lows on either side. Surface high delineated by pecked isobar. EABR had commenced formation a few days earlier. Lower tropospheric Monsoon Trough (MT) in normal position. Stage 3, EABR had intensified along with weakening of WABR. Low upstream of the EABR shifts southwards. Stage 4, Monsoon trough is displaced significantly northwards leading to monsoon break.